Original Article

Special Issue on *Disaster Risk Reduction in Mountain Areas*

Early landslide mapping with slope units division and multi-scale object-based image analysis – A case study in the Xianshui River basin of Sichuan, China

GAO Hui[1,2,3] https://orcid.org/0000-0002-9992-1656; e-mail: sandygao2008@126.com

HE Li[1,4]* https://orcid.org/0000-0002-1362-8310; ✉e-mail: heli2020@cdut.edu.cn

HE Zheng-wei[1,2]* https://orcid.org/0000-0001-7690-2949; ✉e-mail: hzw@cdut.edu.cn

BAI Wen-qian[1,2] https://orcid.org/0000-0001-9629-475X; e-mail: baiwenqian@stu.cdut.edu.cn

*Corresponding author

1 State Key Laboratory of Geohazard Prevention and Geoenvironment Protection, Chengdu University of Technology, Chengdu 610059, China

2 College of Earth Sciences, Chengdu University of Technology, Chengdu 610059, China

3 Chengdu Center, China Geological Survey, Chengdu 610081, China

4 College of Tourism and Urban-Rural Planning, Chengdu University of Technology, Chengdu 610059, China

Abstract: Previous studies on optical remote sensing mapping of landslides mainly focused on new landslides that have occurred, but little attention was paid to the early landslide due to its high concealment. InSAR technology, a prevalent method to detect early landslides, only can be used to identify the potential hazards of slow deformation. Therefore, it is necessary to explore new method of early landslides mapping by integrating all types of direct and indirect early features, such as cracks on slopes, small collapses inside and topographic features. In this study, an object-oriented image analysis method based on slope unit division and multi-scale segmentation was proposed to obtain accurate location and boundary extraction of early landslides. In the middle- and small-scale segmentation, the object, texture, spectrum, geometric features, topographic features, and other features were obtained to determine the local feature location of early landslides. The slope unit boundary was combined with the feature of a large-scale segmentation object to determine the scope of landslides. This method was tested in the Xianshui River basin in the Daofu County, Sichuan Province, China. The results demonstrate that: (1) Such features as landslide cracks and the small collapse at the bottom of slope can effectively determine the landslide position. (2) The slope unit division and the correct setting of shape factors in multiple segmentation can effectively determine the landslide boundary. (3) The accuracy of landslide location extraction was 83.33%, and the accuracy of boundary extraction for early landslides that were completely identified was evaluated as 82.67%. It is indicated that this method can improve the accuracy of boundary extraction and meet the requirements of the early landslides mapping.

1 Introduction

Landslides can be triggered by several factors, such as global warming, abnormal climates, earthquakes (Fan et al. 2019), and the increase of infrastructure construction in mountainous areas. Monitoring and observing landslides and the early identification of risks are crucial for reducing the damage caused by their occurrence. Remote sensing can be used as an essential survey tool to identify the exact location and the landslide risk areas in the early stages. The early stage of landslides is the period before the overall sliding of a slope without landslide history or before the restoration of a previous landslide with many hidden characteristics. The existing remote sensing data types for identifying the early hidden dangers of landslides mainly include the following three categories: optical remote sensing image, InSAR technology and airborne LiDAR.

Identifying new landslides using the existing optical remote sensing data has become quite an advanced process now; there are several classification methods. For instance, the data can be categorised based on the changes in optical images before and after landslides (Chen et al. 2018; Huang et al. 2020). The unsupervised classification can be used to observe the changes by landslides (Tran et al. 2019; Wan et al. 2015), whereas machine and deep learnings can be integrated to detect landslides (Bui et al. 2020; Lei et al. 2019; Liu et al. 2021; Lu et al. 2020; Zhang et al. 2020; Zhu et al. 2020). The effectiveness of these methods and technologies has been demonstrated in identifying large-scale new landslides that arise rapidly due to earthquakes such as the Wenchuan and Jiuzhaigou earthquakes (Dong et al. 2020) and the rainfall precipitation (Liu et al. 2020; Miura and Nagai 2020). However, effective methods are inadequate to detect the early stages of new landslides due to the high degree of concealment in the early stages. Furthermore, because existing approaches identify only a few landslide element characteristics and an imprecise overall form, it is impossible to establish its continuous edge.

InSAR technology is an effective and essential means for identifying and discovering geological hazards that induce deformation. This technology has demonstrated remarkable application effects in recent years (Hu et al. 2020; Yang et al. 2021; Li et al. 2018; Liu et al. 2019; Acosta et al. 2021; Acosta et al. 2021; Esposito et al. 2020; Syzdykbayev et al. 2020). Airborne LiDAR can readily identify and discover old landslide collapse deposits and other loose deposits of various causes by using the real terrain after vegetation removal (Syzdykbayev et al. 2020; Gazibara et al. 2019; Miandad et al. 2020). Although the above method has been widely used, it still has several shortcomings (Lissak et al. 2020). InSAR can only be used to identify the potential hazards of slow deformation. In addition, regional "deformed slope target area" and landslide deformation rate are also identified, which will be affected by vegetation coverage, data processing and detection cycle. Complex terrain and vegetation will lead to an incoherence phenomenon; hence, InSAR cannot identify the old landslide that has been in a stable stage and has no sign of sliding. The interpretation accuracy is also related to the interpreter's personal experience. Airborne LiDAR also has high costs and is not suitable for applications in large areas (Xu et al. 2019)

In summary, as a stable and widely used data type, it is necessary to explore the value of optical remote sensing data in the early stage of landslides to identify hidden dangers. The object-oriented image analysis (OBIA) method was implemented successfully in various fields (Bui et al. 2020; Chen 2017; Liang and Zhang 2020; Lopes et al. 2021; Luo 2021; Oreti 2021; Șerban et al. 2021; Zhao et al. 2020). Keyport et al. (2018) studied and compared two analysis methods based on pixels and objects in 2017. The use of optical images for detecting the characteristics depicting the early formation of landslides can be described as the process of reasoning based on the indirect signs of landslides gathered by previous researchers. Simultaneously, OBIA is more similar to a human cognition process that is based on the knowledge and experience, in which the indirect signs are represented using indices and information, such as primary data, remote sensing images, spatial and semantic relationships of surface characteristics (Martha et al. 2011). These characteristics are integrated to avoid the phenomenon of similar objects with different spectra and things with similar ranges.

In the study of object-oriented extraction of landslide characteristics of landslide body, Chen et al. (2017) used zY-3 satellite's spectral information and

derivative products of DEM to obtain layer information, texture and geometric features based on random forest (RF) and mathematical morphology (MM) to conduct object-oriented landslide mapping. Kurtz et al. (2014) used remote sensing data at different resolutions (middle to ultra-high key) coupled with DTM data to perform multi-layer landslide data extraction from top to down area. All the above researchers have conducted relevant research on the topographic features of landslides themselves. However, due to the relatively weak information on the early hidden dangers of landslide, the incomplete features in the form of some hidden dangers of landslide, and the inadequate study on the characteristics of landslide itself, the researchers have been able to come up with a suitable method. In addition, the feature research object is extended to the whole slope unit of landslide breeding, which provides the possibility to obtain more useful object features.

The aforementioned literature review showed that the OBIA combined with optical sensing data had a strong application prospect for detecting the formation of landslides. Thus, the OBIA method is used in this paper to automatically extract the early signs of landslides from remote sensing data. This study is based on previous research and knowledge of how landslides develop and distribute in the study area. Local feature extraction is used to prove the existence of the whole landslide. Then, slope units are used to limit the scope of landslides. Based on the completion of multiple segmentation on different scales, classification is performed to complete the accurate extraction of the target. This method can not only extract the old landslide with a complete boundary but also locate the slope elements with landslide characteristics, significantly improving the accuracy and efficiency of early landslide extraction.

2   Materials and Methods
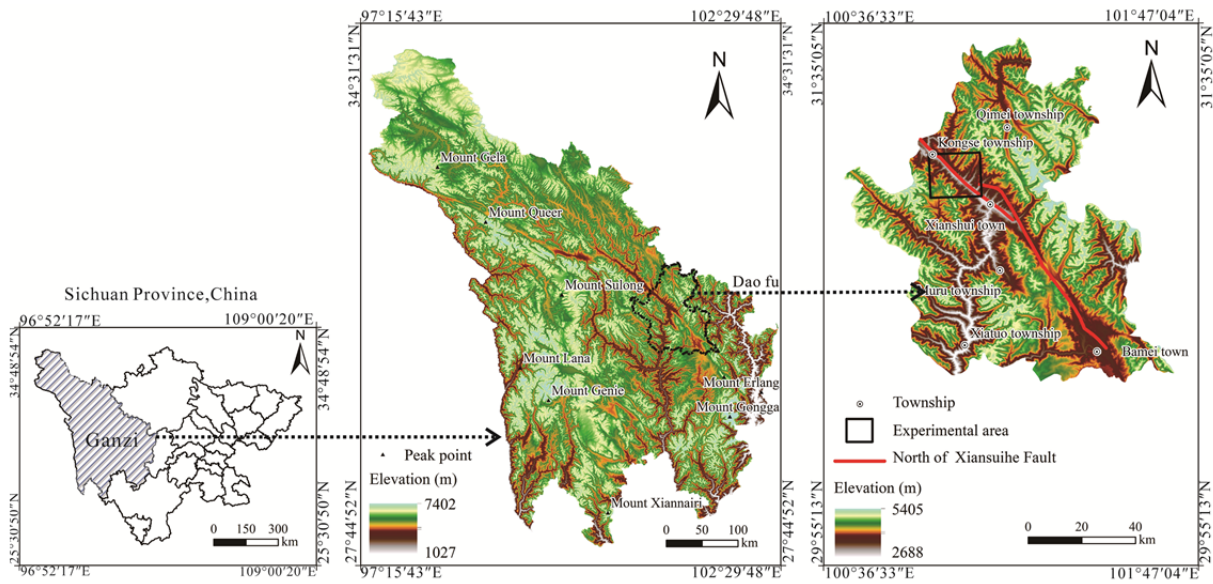
2.1 Study Area

The studied region for this research was the Xianshui River basin at an altitude of 4,172−2,655 m, located in the southeast foot of the Tibetan plateau and bounded by the northeast edge of the Hengduan mountains. This area lies in the transitional zone from a hilly to a mountainous plateau between the Daxue and Shaluli mountains. The topography of the study area is controlled by regional geological tectonics that is observed through the ridges that mainly extend along tectonic lines (Guo et al. 2015, Duan et al. 2005). The rotating broad valleys and gorges govern the basin's middle and upper reaches. The wide valleys contain alluvial graben basins that produce beads threaded into a string. Flood plains and river islands are developed because of the broadness of the riverbed. The gorges are high and narrow, with steep slopes generally at the gradient of 25°–40° and even more than 40° in local areas. The fracture zone of Xianshui River in the basin continues from the Donggu town within the Ganzi county located in the north to the Longden town within the Daofu county situated in the south. It cuts across the middle and upper reaches of the Xianshui River in the northwest (NW) and the southeast (SE) direction. A large sinistral strike-slip fracture zone is considered active up to date, with earthquakes often occurring in this zone.

Meanwhile, rocks and earth elements are severely broken along the fracture zone, and the fracture zone can even extend hundreds to thousands of metres in width in local areas. Severe geological hazards such as large-scale landslides and debris flows may happen due to earthquakes, fault creeps and heavy rains, leading to loss of massive budgets (Guo et al. 2015). Earthquakes and early landslides cause many old and paleo landslides because of the creep of faults and permafrost (Yao et al. 2017). This activity was evident in the database of the existing geological hazards, visual interpretation and InSAR-related work. Therefore, the landslides in the Xianshui River basin represent the mountainous area of Southwest China. This basin area was chosen as the study area of this research (Fig. 1).

2.2 Data Sources

This study's primary data comprised remote sensing optical image and topographical data. The image data were captured by the Chinese GF-1 satellite that recorded panchromatic accurate colour fuse data having a resolution of 2 m. Those data were obtained on 19 November 2017 from the Geocloud platform of China Geological Survey, a free system that provides remote sensing data service and can be accessed at: http://geogf.agrs.cn/search. The topographical data were obtained from the ALOS DEM data having a resolution of 12 m that were

Fig. 1 Location of the study area: Daofu County, Ganzi Tibetan Autonomous Prefecture, Sichuan Province, China.

provided for free from the official website of NASA available at: https://search.earthdata.nasa.gov/search. The DEM data were mainly used for the orthorectification of image data. These data were also used to obtain information for the slope, aspect, slope unit and distances in river networks to assist in extracting the landslide-related information. The known landslide hazard points in the study area are used as the sample for early landslide mapping, of which 60% are used as the training set and 40% are used as the validation set (Fig. 2). The Geocloud platform of the China Geological Survey provides the known landslide hazard points. Notably, the landslide with no visual interpretation due to shadow and trees was not included in the sample set.

2.3 Early Characteristics of Landslides

The image characteristics and spatial distribution of early landslides were analysed using previous researchers' (literature) expertise and the collected characteristics for early landslide samples in the study area.

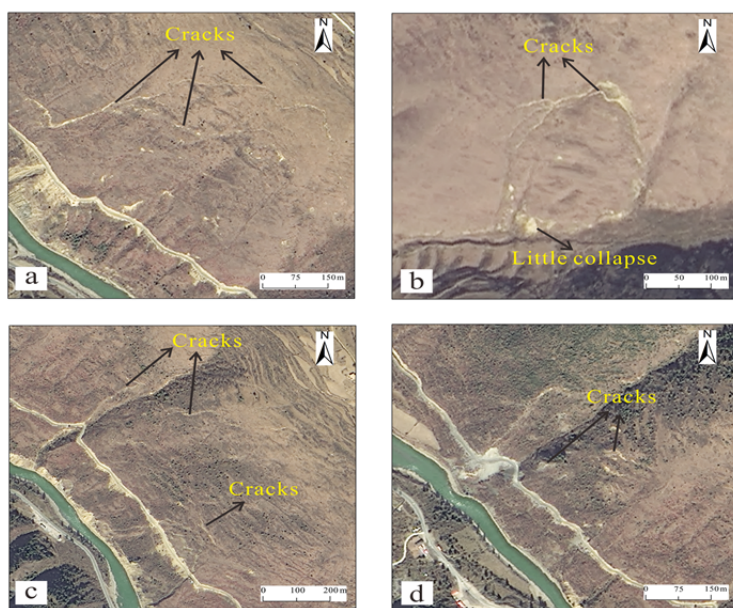#### 2.3.1 Image Characteristics of Early Landslides

Landslides in the study area were divided into two types based on their landslide history and were investigated separately.

The fractures appearing on the slopes, which comprise tension, expansion and shear fractures, are the primary image indicators of landslides for slopes
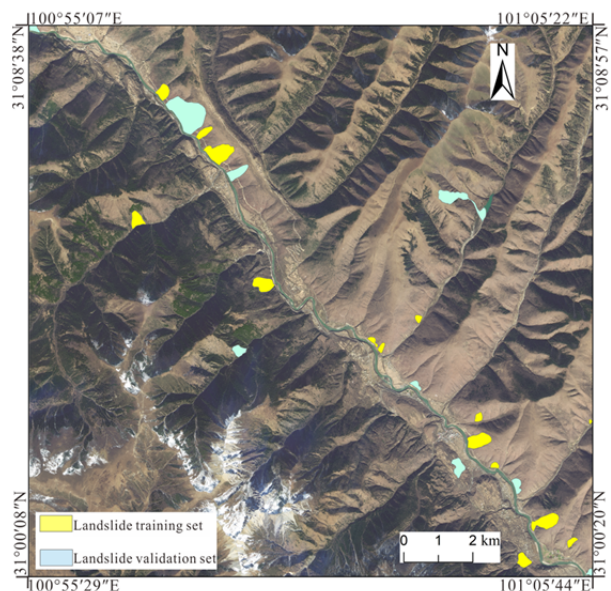
Fig. 2 Landslide training set and landslide verification set in the study area.

without large sliding areas (Fig. 3). These fractures were divided into horizontal fractures at the rear side, radiating fractures within the slope body and vertical fractures on both sides. The number of fractures varied as the landslide progressed through various stages. Faults could have continuous or discrete boundaries, and there might be only one indication in some cases. Because of no continuous fracture surface formation in the early stage of landslides, the risk of landslides could only be assessed based on the fractures' location, strike, and density. Its development trend would depend on the effect of the

Fig. 3 Image signs and characteristics of early landslides. (a) and (b) Boundary comprises discontinuous cracks; (c) and (d) No clear boundary.
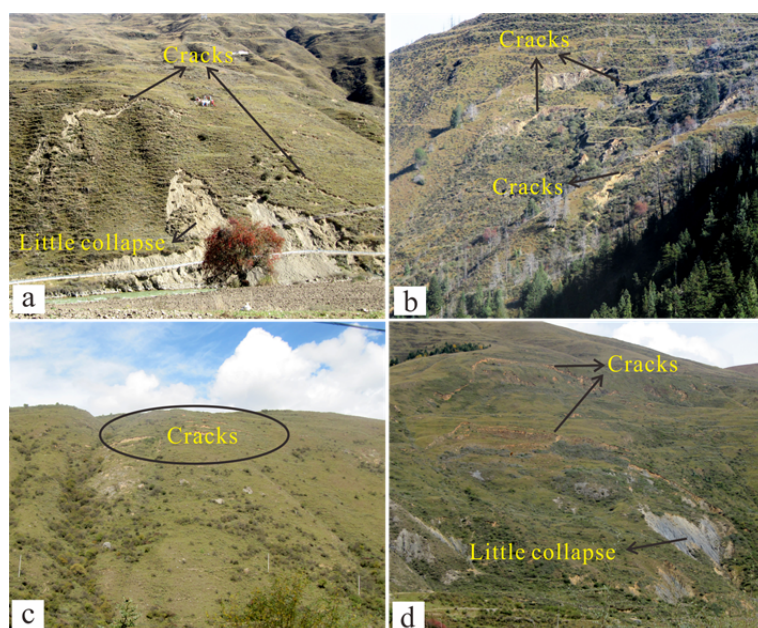
Fig. 4 Field identification marks of early landslides. (a) and (d) Boundary cracks coexist with the slope foot collapse on the landslide; (b) Abnormal depressions formed by cracks; (c) Transverse cracks in the state of creeping deformation.

topography. Fractures were depicted in the images by bright linear areas created by exposed rocks and earth materials. Shades as plants or rocks covered the abnormal cavities and steep banks were formed when the ground surface was broken (the latter was observed mainly in vegetated areas). In either case, striking differences existed between fractures and

background objects in terms of spectrum, texture and shape preconditions for further extraction. Besides, some deposits at the foot of the slopes were also considered as indicators of landslides, which were mainly depicted in the images by small bright areas. Field photos presented in Fig. 4 show the section from Daofu to Luhuo of the Xianshui River fracture zone. The early signs of landslides were presented on the images to clearly depict the characteristics of early landslides.

Original characteristics of landslides were fully or partially preserved in the areas where there was an indication of previous large-scale landslides. Fig. 5 shows that the type with complete landslide elements was easily detected. This type of landslides had clear and thorough boundaries; moreover, tongue-like shapes and continuous bright areas were also observed in this type. Landslides occurred a long time ago in some human settlements where deposits at the front of landslides mainly developed into farmland or residential areas because of their flat terrains. Topographical data such as LiDAR high-resolution data were primarily used to identify landslides because of the difficulty in recognising their surface characteristics within the images (Fan et al. 2021), and these ancient landslides does not belong to the research category of this paper.

2.3.2 Characterisation of Spatial Distribution for Landslides in the Study Area

The distribution of landslides has a significant impact on their origins. The internal roots affecting the formation of landslides are geographical environment, topography, geological background and climatic conditions. Besides, landslides are also triggered by earthquakes, rainfall and human activities (Kusumawati et al. 2017). The geological hazards in the Xianshui River basin are usually distributed in linear patterns or clusters within zones or areas. For instance, some risks are present along traffic arteries, rivers or valleys, or in regions by
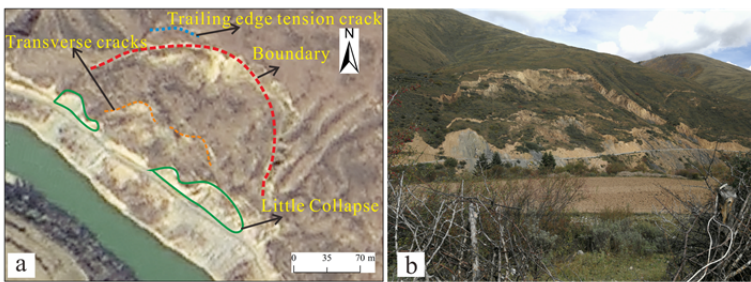
Fig. 5 Typical old landslides formed because of earthquakes and comparison of field photos. (a) Image identification sign of ancient landslide; (b) Old landslide field photo.

townships, villages and mines. Landslides in the Xianshui River basin typically occur at an elevation of 2,600–4,000 m with a slope angle of 20°–50°. The slopes in this area are mostly transverse and oblique. The slopes categorised as unstable mostly have a slope angle of 30°–60°.

Landslide risk zones were categorised into two types based on the analysis of the landslides conducted in this study. The first type concerns the rivers controlled by distance from waterways, locations relative to river bends and the bank type of rivers (convex or concave). The second type was associated with the topographical characteristics such as elevation, slope type, gradient and aspect. They were just important factors for aspect and slope type and cannot be used quantitatively. Therefore, elevation, slope and distance from rivers were only chosen as significant factors contributing to the distribution of landslides.

2.4 Methods

The framework depicted comprised three parts: extraction of local characteristics, division of slope units and extraction of landslide boundaries. A separate object-oriented classification project assisted in obtaining the results of each section. Local characteristics were extracted using GF-1 image and DEM data to segment images and to obtain the object. Object and landslide listings are then integrated to mark the local characteristics, establish a threshold classification, and validate the method using the hold-out method, with 60% used as the training dataset and 40% used as the verification dataset. Slope unit division provided the image segmentation result of the slope direction graph, which is used as the basic file of landslide boundary extraction after smoothing and removing flat land. Extraction using slope

landslide boundary is obtained after image segmentation. The objects were combined with local characteristics to obtain the candidate slope. However, image segmentation was done again for candidate slope to obtain a new object. The landslide was marked by combining the object and landslide lists. Then, the threshold classification was established. The method verification was consistent with local feature extraction. Finally, the accuracy of the results was evaluated.

2.4.1 Pretreatment of Basic Data

The image and topographical data were the primary data used in this study. The image data comprise GF-1 panchromatic accurate colour fuse data and texture data with a resolution of 2 m. The topographical information comprised the ALOS DEM data with a resolution of 12 m, slope aspect, slope gradient and distance from the rivers obtained from DEM data (Fig. 6). GF-1 data were pretreated using
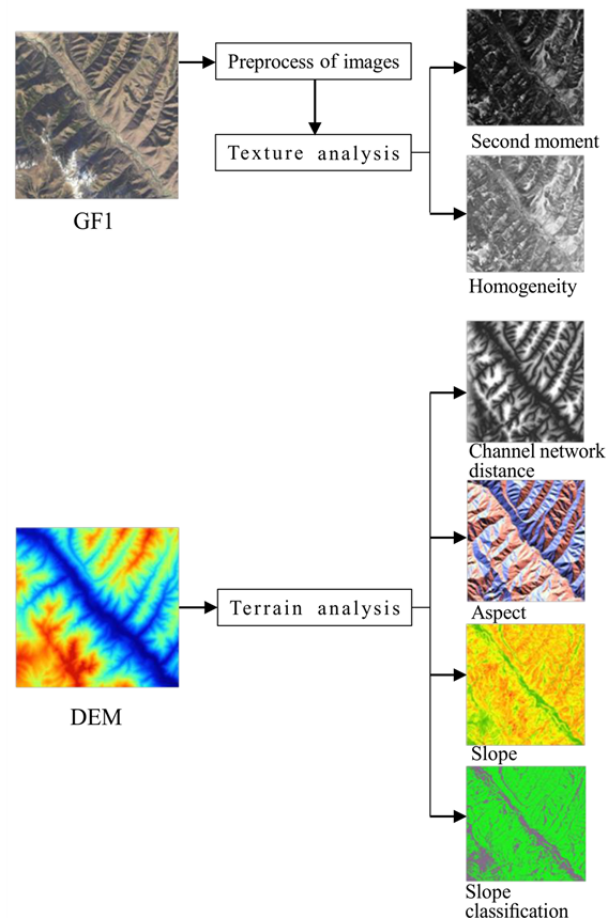
Fig. 6 Diagram of elemental data composition.

the ENVI software that involved radiometric correction, atmospheric correction, orthorectification, and the fusion of panchromatic and multispectral data. The texture analysis of remote sensing optical images was finalised using ENVI for a shorter computation time. Then, the texture results were used as a distinct layer in eCognition for subsequent classification calculations. SAGA provided the maps of aspect and distance from rivers, whereas ArcGIS was used to reclassify aspect and slope for the topographical data. The aspect map was mainly used for extracting slope units.

2.4.2 Local Characteristics Extraction Method

Local feature extraction comprises two image segmentation and two threshold classification processes. The purpose of two segmentation processes was to solve the problem of long calculation times caused by small-scale segmentation in large areas and to fulfil the requirements of extraction targets in different stages. The principle of image segmentation was used to ensure that extracted objects had a proper size to cluster the characteristics effectively. The first image segmentation was conducted on a medium scale, which was selected according to the DEM and image resolution. The second segmentation process was performed on a smaller scale to obtain more detailed location information. The object property parameters of the homogeneity coefficient were optimised through multiple tests. Because damages to the surface were used to characterise the early stage of landslides, the colours and textures of the original cover were changed in specific directions, resulting in mottled directional textures. Based on the abovementioned reasons, the shape factor should be appropriately increased to prevent the segmentation results from being too broken.

Threshold classification uses the assignment class algorithm in eCognition that uses a criterion to determine whether an image object belongs to a class. The method of obtaining the threshold is as follows. The samples were obtained by manual calibration after referring to the position of the known landslide training set, that is, samples of the same scale were obtained after each segmentation. Then, the statistical results of the sample feature information were used to set a reasonable threshold.

Selection of object characteristics, the early landslide features were mainly exposed rock soil that formed radial and strip textures. The initial range of local information was obtained through elevation, slope, spectrum, and threshold classification of texture information. In addition, interference factors such as roads were preliminarily eliminated. For small-scale objects, fractures were considered a vital shape factor, and the difference in spectral characteristics between objects and backgrounds was more striking on a smaller scale. Hence, the shape index and average spectrum data of adjacent things were added to identify the deposits at the bottom of the slope and fractures (Fig. 7).

2.4.3 Slope Unit Extraction Method

The purpose of extracting slope units is to use the slope element's boundary to define the effective boundary of landslides. A new method is proposed for the faster extraction of slope units. This method uses the SAGA slope to the aspect map and converts it into colour raster images, which are widened to figure visual differences using multi-scale segmentation for quickly obtaining the slope unit. The slope boundaries were smoothed using ArcGIS to avoid the jagged borders triggered because the DEM has a lower resolution than image data resolution. Finally, the ultimate limits of the slope units were obtained after
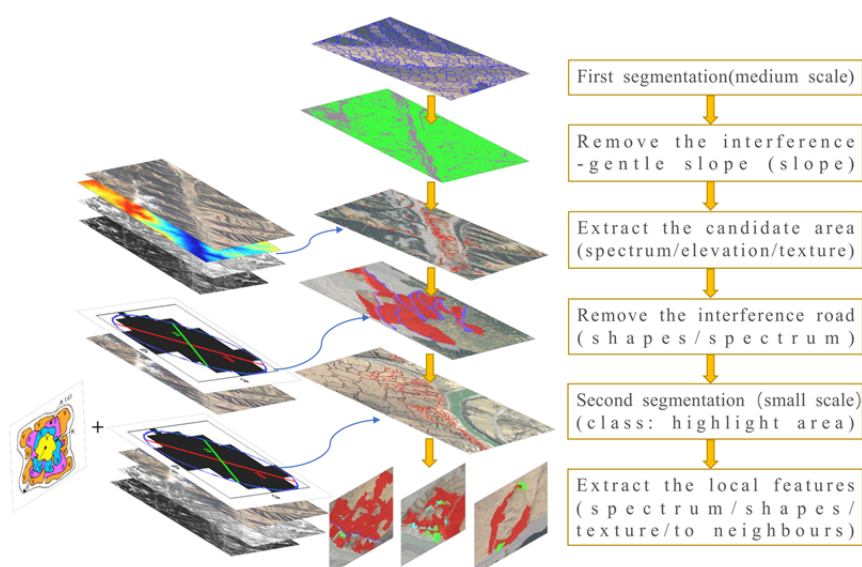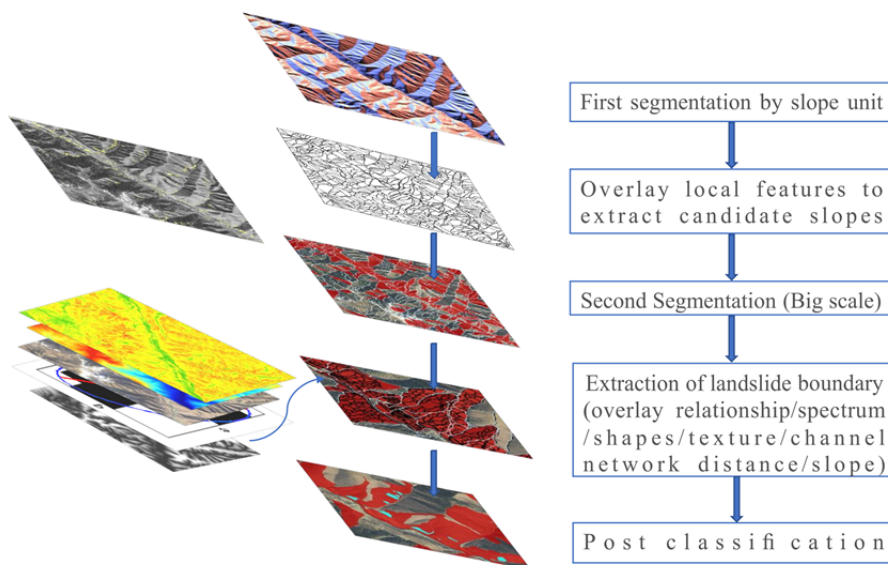

Fig. 7 Flowchart of early local feature extraction.

removing the flat areas such as river valleys. The shape and tightness factors were the critical factors of the multi-scale segmentation. The colourful raster image of the aspect shows the variation of micro-topography in a sloped unit that led to changes in aspect and resulted in colouring differences. Therefore, a reasonable scale slope element can be obtained after repeated tests by increasing the shape factor and reducing the compactness factor.

2.4.4 Early Landslide Boundary Extraction

The overall boundary of early landslides was determined after two rounds of segmentation by classification. First, the vector boundaries of slope units were adopted to segment images and the local information of slopes was superimposed on the slope units to obtain the candidate slope units.

In the second step, multiple-scale segmentation was used to produce slope units. In this process, the shape factor should be appropriately increased to ensure the shape's integrity. Moreover, the overall boundary was achieved using the threshold classification and the overlapping relationships between fractures and deposits. Segmented objects in slope units, spectral characteristics of things, distance from rivers, slope, factor indicator, etc., were also used to determine the overall boundary (Fig. 8). Nevertheless, post-classification treatments, for instance, amalgamation, were also used to determine the early landslide boundary.
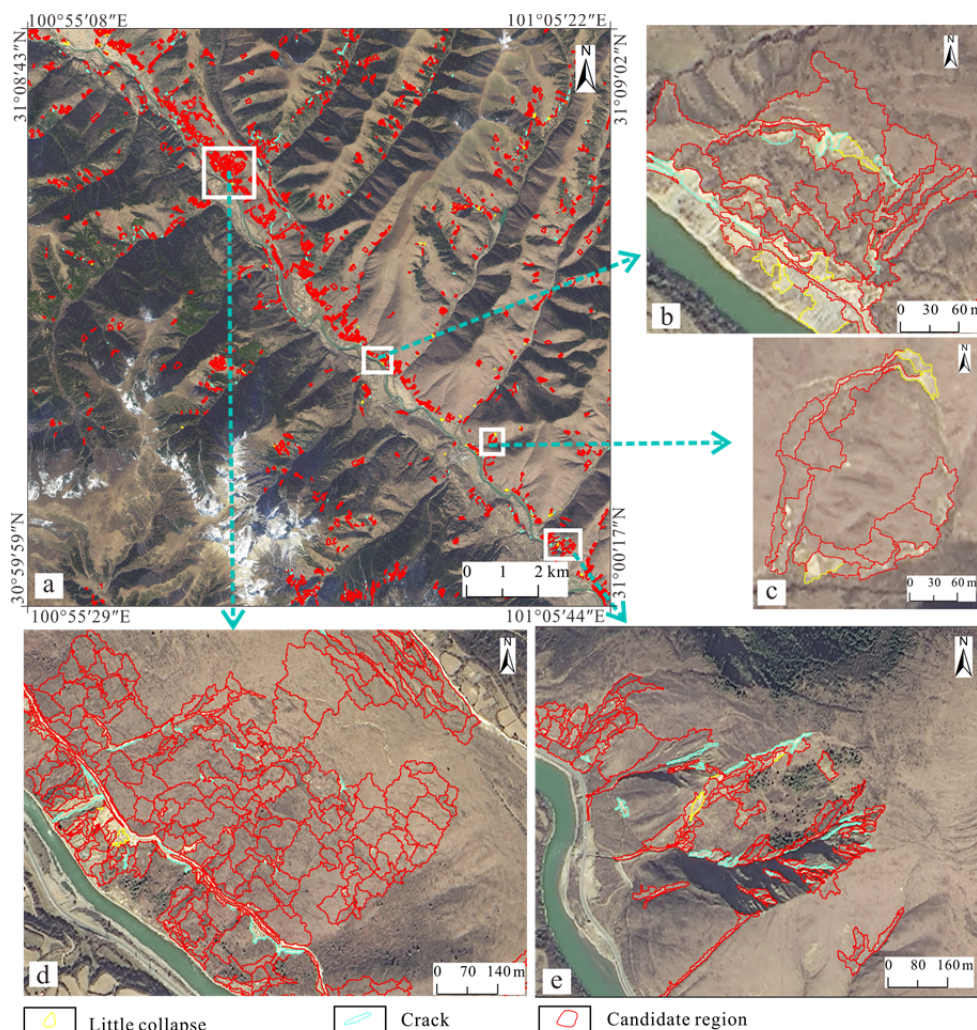
3   Results

3.1 Extracting Early Local Characteristics

Two rounds of image segmentation and threshold classification were used to finalise the local characteristics of early landslides. First, GF-1 accurate colour data were segmented at a medium scale of 100 and a shape factor of 0.5. After obtaining segmentation results, gentle areas were removed first. The removal results showed that most of the removed areas were human engineering projects, such as roads, buildings and farmland. Because such features are similar to small collapses in spectral characteristics, eliminating gentle areas can effectively reduce disturbances. The maximum spectral value of the red band, two texture feature indices and elevation values were combined to determine the preliminary scope of early landslides. The areas that included the early landslides were described as bright areas. However, the bright areas only accounted for 2.84% of the whole area, effectively reducing the amount of calculation. The selection of maximum pixel values rather than mean values in spectral features is the main reason to ensure that small areas are not missed. The density and asymmetry index effectively reduce road disturbance in sloping areas.

The early chosen areas were initially segmented for the second time at a scale of 50 and a shape factor of 0.5. Segmentation results showed that the decrease of the effective scale highlighted the discontinuous cracks. The extraction results of small collapses showed that the feature of mean difference from neighbouring objects is the key to obtaining collapses. This feature further highlights the differences between cracks and background, rather than simply identifying them from their own brightness. (Table 1 and Fig. 9).

The extraction results for the local characteristics could still be affected by other objects. The first influential factor was the paths to mountains whose spectra and shape were very similar to

Fig. 8 Flowchart depicting the extraction of early landslide boundary.

Fig. 9 Extraction results for early local characteristics. (a) Early local feature extraction results of landslides in the whole study area; (b) Local feature extraction results of old landslides; (c), (d) and (e) Early local feature extraction results of the landslide monomer.

Table 1 Process of extraction for local characteristics of early landslides

Execution order	Objective	Scope	Characteristics and processes
1	First medium-scale image segmentation for the first level	Pixel level	Multi-scale segmentation algorithm.
2	Extraction of candidate regions	New level	The classification was based on the thresholds of two textural features of homogeneity and second moment. For the maximum pixel value in the red waveband, the roads were removed for the threshold's classification of density, asymmetry and shape index.
3	Second small-scale image segmentation of the first level	New level	Multi-scale segmentation algorithm
4	Fracture extraction	New level	The classification was based on the thresholds of average spectral value in the waveband, shade index and asymmetry.
5	Small deposits extraction	New level	The classification was based on the thresholds of average spectral value in the waveband, a moderate difference from adjacent objects and second moment.

those of fractures. They were all long strips that might also be present in the steep areas or even landslides.

Small deposits might exist on the sides of the pathways. Therefore, eliminating the paths based on

such characteristics is highly complex.

Furthermore, the second interference is ridges on farmlands whose spectra and shape resemble fractures. Besides, creeping abandoned farmlands within the study area made it challenging to avoid ridges. The ridges might be mistakenly considered as small deposits in farmlands with a significant slope. The spectra of farmlands resembled that of bare earth as the data were obtained during Autumn and Winter. To be precise, this is the phenomenon of different objects with identical spectra. Some cases of misjudgement could be corrected after identifying the overall boundary of landslides.

3.2 Extracting Slope Units

The aspect map created from DEM data with a resolution of 12 m was converted into an RGB colour raster map (Fig. 10a). Then, the multi-scale segmentation was performed at a segmentation scale of 50, a shape factor of 0.9 and a tightness factor of 0.1. The segmentation results were transferred using eCognition to a vector file (Fig. 10b) and were smoothed in ArcGIS (Fig. 10a). Fig.10c shows the file of the existing river valley used to exclude the flat fluvial areas that were primarily governed by mountains in the study area. The experimental results demonstrate that this method could quickly identify the slope units' boundaries suitable for high mountainous regions. Furthermore, the scale of extraction used for slope could be flexibly adjusted, providing a good foundation for the subsequent rapid detection of landslides and extracting the overall boundary.
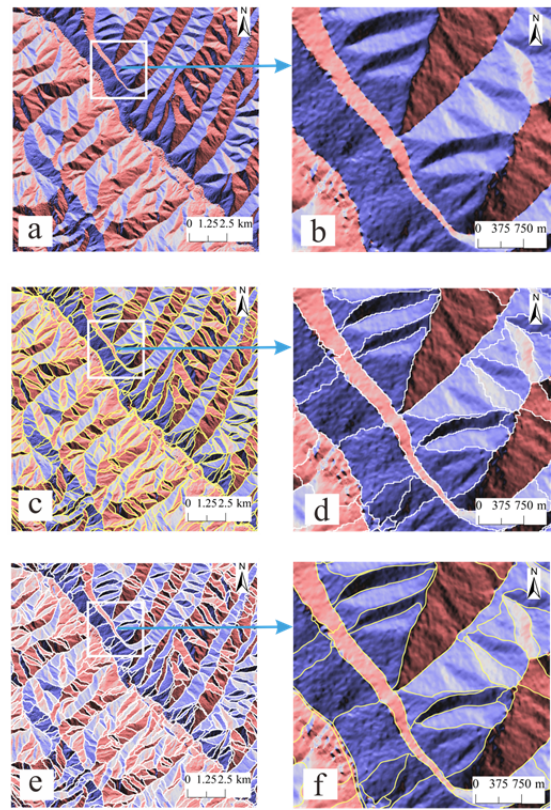
Fig. 10 Slope extraction process. (a) Aspect map; (b) Part of the aspect map; (c) Preliminary results of slope units; (d) Part of preliminary results of slope units; (e) Final result of slope units; (f) Part of final result of slope units.

3.3 Extracting the Overall Boundary

The image's chessboard segmentation was conducted using slope unit boundaries, and the candidate slope was obtained by superimposing local landslide characteristics and defining the slope gradient (Fig. 11a). Then, the candidate slope was subjected to secondary multi-scale segmentation (Fig.

Table 2 Extraction processes for the overall boundary

Executive order	Objective	Scope	Characteristics and processes
1	The first image segmentation of the second level	Pixel level	The chessboard segmentation algorithm with a sufficiently large scale of about 1,000,000 was used. The segmentation was based on the vector file of the slope units.
2	Extraction of candidate slopes	New level	The classification was done according to the thresholds of overlaid local characteristic vectors and slopes.
3	Second large-scale image segmentation of the second level	New level	The multi-scale segmentation algorithm was used with a scale of 200, a shape factor of 0.5, and segmented objects of candidate slopes.
4	Extracting the overall boundary of the early landslides	New level	The classification was based on the thresholds of the number of overlays, maximum overlay proportion, slope, elevation, distance from rivers, homogeneity, shape index, asymmetry, pixel maximum, means and area of an object.

11b) at a segmentation scale of 200 and a shape factor of 0.5. The object features mainly include the number of overlays, maximum overlay proportion, slope, elevation, distance from rivers, homogeneity, shape index, asymmetry, maximum pixel, means and area of an object (Table 2). The results indicated the existence of two types of landslides in the study area. There were two types of shapes for the early landslides that were extracted. One of the types includes the complete shapes of landslides with fully identified boundaries (Fig. 11d–f). The other type referred to the local shapes of early landslides whose boundaries were not fully recognised. The first is that the area of the segmentation object is large and the distribution is concentrated; however, the number is small. The second is that the local features are small and scattered, accounting for a small area of the whole segmentation object, whereas the number is large. For these two different cases, the first one mainly relies on the maximum stacking percentage of local features and segmented objects. In contrast, the second one depends on the stacking number to determine whether it is the final extracted object. For instance, Fig. 11g only reveals the shape of the lower part of the landslide because its right boundary was not as clear as the left boundary. Figure 12-h shows that the slope toe collapse of landslides was mainly extracted. Visual interpretation can roughly outline the shape, but it is challenging to aggregate it into a whole due to the slight difference between the object and its surroundings. It should be noted that the adjacent landslides would be merged in the post-processing of the merged boundary; therefore, the results of the two categories of class merged and
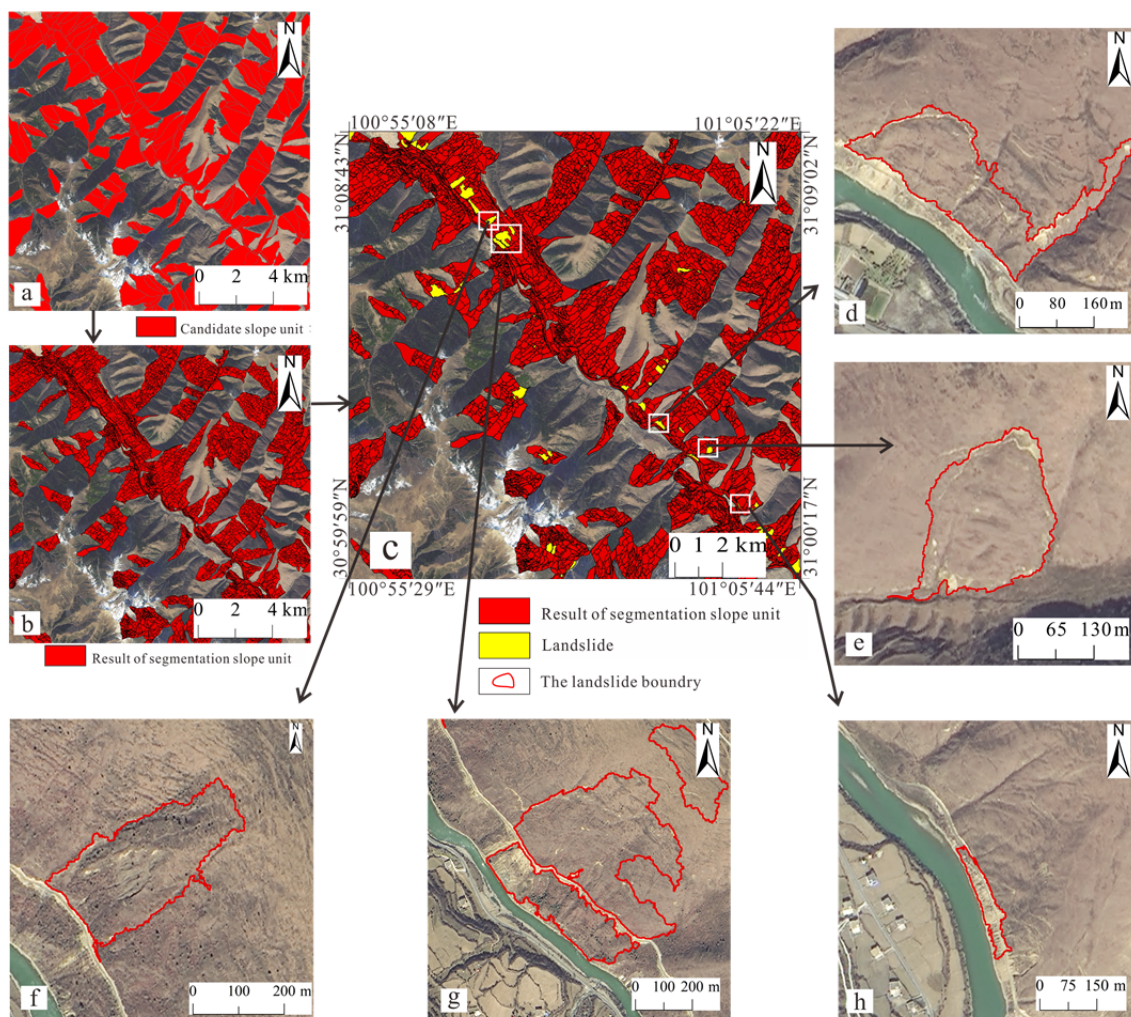
Fig. 11 Overall boundaries of earth landslides. (a) Results of candidate slope unit extraction. The result (b) is obtained by multi-scale segmentation of (a), and The Final extraction result (c) is based on the classification of (b). (d), (e) and (f) are the complete landslide boundaries, (g) and (h) are incomplete landslide boundaries.

unmerged (Fig.11d, Fig.12f) were retained as the merged results.

3.4 Accuracy Assessment

Two tests were performed to assess this study's methodology. First, the success rate of landslide extraction was evaluated. Second, the OBIA methodology was tested against independent landslide information (Fig. 12). The extracted landslide was superimposed with the training dataset and verification dataset obtained by visual interpretation, respectively, to obtain the part with the same position. The number of superimposed and the proportion of data set were calculated to obtain the accuracy of landslide location extraction. The

detection performance achieved the rate of 86.6% with the training dataset and 77% with the validation dataset in successfully detecting landslides. Finally, 83.33% of landslides were successfully mapped for the total sample set.

$$\text{Location Accuracy} = N_m/N_{gt} \qquad (1)$$

N_m represents the total number of the mapped landslides that are matched with the ground truth, N_{gt} represents the total number of the ground truth.

For the landslide with complete landslide boundary, representative landslides were selected. The confusion matrix and Kappa coefficient were calculated to evaluate the accuracy. The extraction accuracy of landslide boundary alone could reach 95.54%, and the Kappa coefficient reached 0.91. The accuracy of boundary extraction for early landslides

□ Automatic Extraction Landslide   □ Visual Interpretation of Landslides
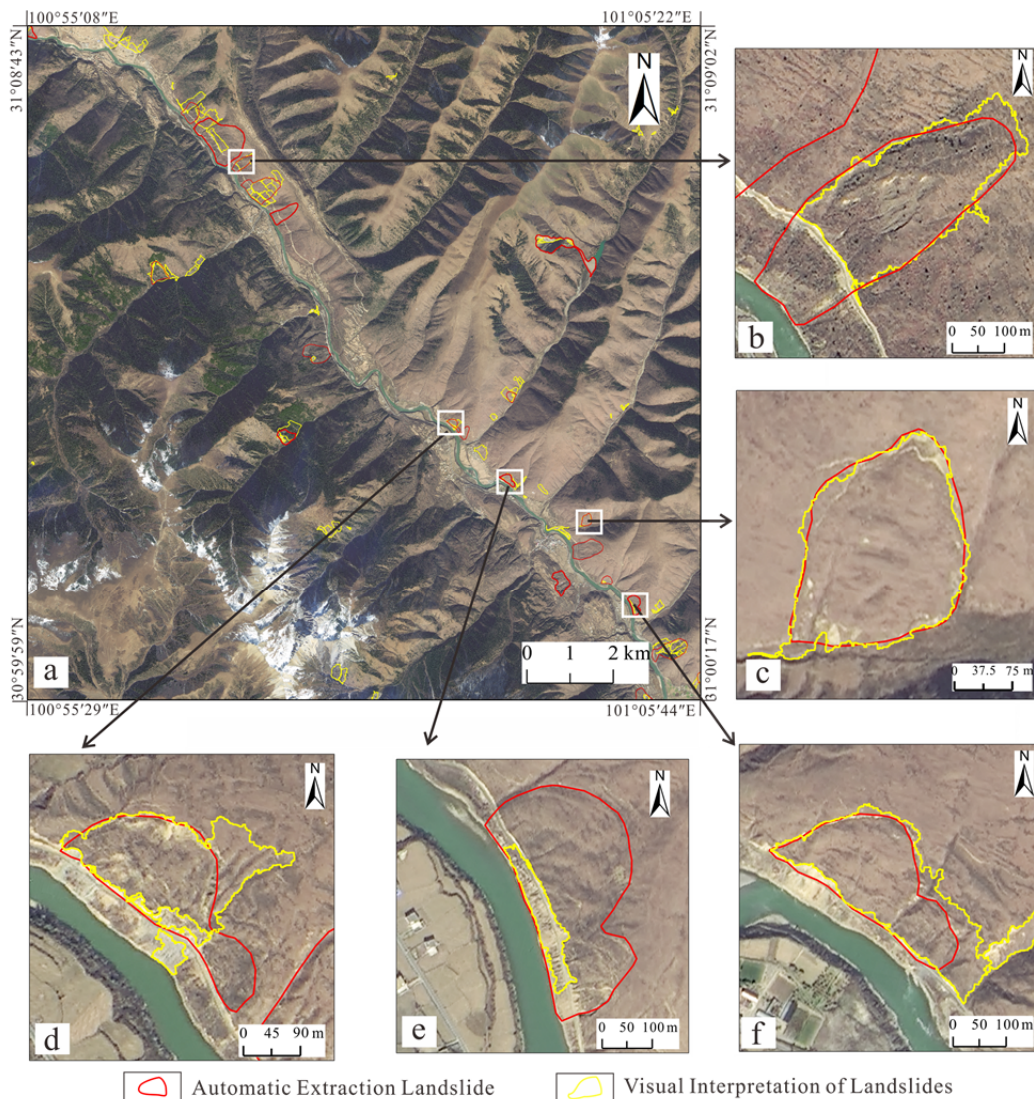
Fig.12 Comparison between automatic extraction results and actual boundaries.

Table 3 Evaluation of accuracy for automatic extraction results of early landslide boundaries

Class	Commission (%)	Omission (%)	Commission (Pixels)	Omission (Pixels)	Prod. Acc. (%)	User Acc. (%)	Prod. Acc (Pixels)	User Acc. (Pixels)
Landslide b	0.00	28.91	0/102715	41772/144487	71.09	100.00	102715/144487	102715/102715
Landslide c	0.00	4.03	0/74135	3116/77251	95.97	100.00	74135/77251	74135/74135
Landslide d	0.00	19.66	0/48042	11756/59798	80.34	100.00	48042/59798	48042/48042
Landslide f	0.00	6.82	0/69610	5097/74707	93.18	1100.00	69610/74707	69610/69610

Note: Prod. = Producer; Acc.= Accuracy.

that were completely identified was evaluated as 82.67%, and the extraction accuracy of typical landslide boundaries was analysed further (Table 3).

4 Discussion

The OBIA classification method was used in this paper to map early landslides. To the authors' best knowledge, no similar paper in this research has been published before. Previous studies had focussed on new landslides whose significant characteristics were obtained from both satellite and UAV images that were spread in continuous large areas (Liu et al. 2021; Lu et al. 2020; Syzdykbayev et al. 2020; Zhang et al. 2020). The early image features of landslides studied in this paper do not have this prominent feature, that is, there is no continuous uniform surface and human cognition can only delineate the early range of landslides by relying on the fissured edge. The multi-scale segmentation method in OBIA software eCognition can rely on adjusting shape factor parameters to solve the problem of extracting patch fragmentation caused by uneven distribution of colour and texture inside the object, to obtain accurate boundary. Previous literature used the same scale for the automatic extraction of different characteristics of landslides (Liu et al. 2021). The multi-segmentation idea of this method can reflect the early characteristics of landslides of different scales. Furthermore, the adoption of multiple scales assisted in saving the computation time and reduced omission errors. Compared with the traditional extraction method proposed by ArcGIS, the technique used in this paper was much more straightforward and accurate in locating boundaries based on a more flexible scale setting. It had different advantages than the MIS-HSU slope extraction method (Wang et al. 2020), which relied on the morphological skeleton. The technique used in this paper was more convenient and less subjected to the effects of small topographical changes. In terms of feature selection, this paper integrated effective information related to landslides from previous studies (Fan et al. 2021; Chen et al. 2017; Dou et al. 2015), mainly including spectrum, shape, texture, topography and other features. Combined with the characteristics of multi-scale segmentation, the feature of spatial superposition relationship between local feature results and large-scale objects is added to strengthen the relationship between local features and the overall landslide.

However, the method used in this paper still has many limitations due to several reasons. Because the extraction of local characteristics is subjected to data resolution, fractures on a tiny scale cannot be extracted. Although data at higher resolution can provide higher accuracy for classification, the total calculation time will be increased accordingly. Hence, the data solution should be chosen based on the specific conditions of the required study area. Furthermore, the selection and setting of classification parameters and their thresholds are based on the distribution law of known hazardous areas chosen as samples for statistics. The choice of samples can have significant effects on extraction results. Hence, the classification accuracy can be improved if more examples are included in the analysis. While considering the choice of thresholds that primarily depends on the subjective judgement of researchers, multiple classification methods can be tested in research. This paper only aims to encourage multiple-scale segmentation to extract landslide characteristics. Researchers can flexibly use multi-scale segmentation to develop various classification methods rather than restrict to a specific classification method.

5 Conclusions

This paper proposed a method to map the early landslide from optical remote sensing data based on the early landslide characteristics and spatial

distribution by using multi-scale segmentation involved in the object-oriented classification and slope unit division. Despite extracting the local attributes of landslides, this method can define the areas at landslide risks through the quick extraction of slope units. It can also improve the accuracy of boundary extraction and meet the demands of the early detection of different types of landslides. Besides, the slope unit extraction method based on image segmentation proposed in the paper is also a rapid and effective extraction method with wide applications. More efforts should be directed towards investigating the application of multi-source data and improving the classification method to expand its application range and extraction accuracy.

References

Acosta G, Rodríguez A, Euillades P, et al. (2021) Detection of active landslides by dinsar in Andean Precordillera of San Juan, Argentina. J South Am Earth Sci 108:103205. https://doi.org/10.1016/j.jsames.2021.103205

Bui TA, Lee PJ, Lum KY, et al. (2020) Deep learning for landslide recognition in Satellite architecture. IEEE Access 8: 143665-143678. https://doi.org/10.1109/ACCESS.2020.3014305

Chen T, Trinder JC, Niu R (2017) Object-oriented landslide mapping using ZY-3 satellite imagery, random forest and mathematical morphology, for the Three-Gorges Reservoir, China. Remote Sens 9(4): 333. https://doi.org/10.3390/rs9040333

Chen Z, Zhang Y, Ouyang C, et al. (2018) Automated landslides detection for mountain cities using multi-temporal remote sensing imagery. Sensors 18(3): 821. https://doi.org/10.3390/s18030821

Dong X, Xu Q, She J, et al. (2020) Preliminary study on interpretation of geological hazards in Jiuzhaigou based on multi-source remote sensing data. Geo Spat Inf Sci 45: 432-441. (In Chinese) https://doi.org/10.13203/j.whugis20190076

Dou J, Chang KT, Chen S, et al. (2015) Automatic case-based reasoning approach for landslide detection: integration of object-oriented image analysis and a genetic algorithm. Remote Sens 7: 4318-4342. https://doi.org/10.3390/rs70404318

Duan L, Zheng W, Li M, et al (2005). Geologic hazards on the western Sichuan plateau and their controls. Sediment Geol Tethyan Geol 25(4): 95-98. (In Chinese) https://doi.org/10.3969/j.issn.1009-3850.2005.04.016

Esposito G, Marchesini I, Mondini AC, et al. (2020) A spaceborne SAR-based procedure to support the detection of landslides. Nat Hazards Earth Syst Sci 20(9): 2379-2395. https://doi.org/10.5194/nhess-20-2379-2020

Fan X, Scaringi G, Korup O, et al. (2019) Earthquake‐induced chains of geologic hazards: Patterns, mechanisms, and impacts. Rev Geophys 57(2): 421-503. https://doi.org/10.1029/2018RG000626

Fan XM, X DL, Zhong YJ, et al. (2021) Recent research on the Diexi paleo-landslide: dam and lacustrine deposits upstream of the Minjiang River, Sichuan, China. Earth Sci Front 28(2): 71. (In Chinese) https://doi.org/10.13745/j.esf.sf.2020.9.2

Gazibara SB, Krka M, Arbanas SM, et al. (2019) Landslide inventory mapping using LiDAR data in the City of Zagreb (Croatia). J maps 15(2): 773-779. https://doi.org/10.1080/17445647.2019.1671906

Guo C, Du Y, Zhang Y, et al. (2015) Geohazard effects of the Xianshuihe fault and characteristics of typical landslides in western Sichuan. Geol Bull CN 34: 121-134. https://doi: CNKI:SUN:ZQYD.0.2015-01-010 (In Chinese)

Hölbling D, Füreder P, Antolini F, et al. (2012) A semi-automated object-based approach for landslide detection validated by persistent scatterer interferometry measures and landslide inventories. Remote Sens 4(5): 1310-1336. https://doi.org/10.3390/rs4051310

Hu X, Bürgmann R, Fielding EJ, Lee H (2020) Internal kinematics of the Slumgullion landslide (USA) from high-resolution UAVSAR InSAR data. Remote Sens Environ 251: 112057. https://doi.org/10.1016/j.rse.2020.112057

Huang F, Chen L, Yin K, et al. (2018) Object-oriented change detection and damage assessment using high-resolution remote sensing images, Tangjiao Landslide, Three Gorges Reservoir, China. Environ Earth Sci 77(5): 183. https://doi.org/10.1007/s12665-018-7334-5

Huang Q, Wang C, Meng Y, et al. (2020) Landslide monitoring using change detection in multitemporal optical imagery. EEE Geosci Remote Sens Lett 17: 312-316. https://doi.org/10.1109/LGRS.2019.2918254

Keyport RN, Oommen T, Martha TR, et al. (2018) A comparative analysis of pixel- and object-based detection of landslides from very high-resolution images. Int J Appl Earth Obs Geoinf 64: 1-11. https://doi.org/10.1016/j.jag.2017.08.015

Kurtz C, Stumpf A, Malet JP, et al. (2014) Hierarchical extraction of landslides from multiresolution remotely sensed optical images. ISPRS Int J Geoinf 87: 122-136. https://doi.org/10.1016/j.isprsjprs.2013.11.003

Kusumawati NA, Putra ID, Wijaya IGNK, et al. (2017) Integrated remote sensing and geological observation in identifying landslide triggering factors: A case study of landslide hazard of Hargotirto Subdistrict, Kulonprogo, D.I. Yogyakarta. Integrated Remote Sensing and Geological Observation in Identifying Landslide Triggering Factors. In AIP Conference Proceedings 1987 (1): 020064. AIP Publishing LLC. https://doi.org/10.1063/1.5047349

Lei T, Zhang Y, Lv Z, et al. (2019) Landslide inventory mapping from bitemporal images using deep convolutional neural networks. IEEE Geosci Remote Sens Lett 16(6): 982-986. https://doi.org/10.1109/LGRS.2018.2889307

Li MH, Zhang L, Shi XG, et al. (2019) Monitoring active motion of the Guobu landslide near the Laxiwa Hydropower Station in China by time-series point-like targets offset tracking. Remote Sens Environ 221: 80-93. https://doi.org/10.1016/j.rse.2018.11.006

Liang H, Zhang M (2020) Object-oriented multiscale deep features for hyperspectral image classification. Int J Remote Sens 41(14):5549-5572.
https://doi.org/10.1080/01431161.2020.1734249

Liu DF, Li JJ. Fan FL (2021) Classification of landslides on the southeastern Tibet Plateau based on transfer learning and limited labelled datasets. Remote Sens Lett 12: 286-295.
https://doi.org/10.1080/2150704X.2021.1890263

Liu P, Wei Y, Wang Q, et al. (2020) Research on post-earthquake landslide extraction algorithm based on improved U-Net model. Remote Sens 12: 894.
https://doi.org/10.3390/rs12050894

Liu XW, Chen Q, Zhao JJ, et al. (2020) The spatial response pattern of coseismic landslides induced by the 2008 Wenchuan earthquake to the surface deformation and Coulomb stress change revealed from InSAR observations. Int J Appl Earth Obs Geoinf 87:102030.
https://doi.org/10.1016/j.jag.2019.102030

Lopes MS, Saldanha DL, Veettil BK (2021) Object-oriented and fuzzy logic classification methods for mapping reforested areas with exotic species in Rio Canoas State Park—Santa Catarina, Brazil. Environ Dev Sustain 23(5): 7791-7807.
https://doi.org/10.1007/s10668-020-00946-0

Lissak C, Bartsch A, De Michele M, et al. (2020) Remote sensing for assessing landslides and associated hazards. Surv Geophys 41(6): 1391-1435.
https://doi.org/10.1007/s10712-020-09609-1

Lu H, Ma L, Fu X, et al. (2020) Landslides information extraction using object-oriented image analysis paradigm based on deep learning and transfer learning. Remote Sens 12(5):752.
https://doi.org/10.3390/rs12050752

Luo C, Qi B, Liu H, et al. (2021) Using time series sentinel-1 images for object-oriented crop classification in Google Earth Engine. Remote Sens 13(4): 561.
https://doi.org/10.3390/rs13040561

Martha TR, Kerle N, Jetten V, et al. (2010) Characterising spectral, spatial and morphometric properties of landslides for semi-automatic detection using object-oriented methods. Geomorphology 116: 24-36.
https://doi.org/10.1016/j.geomorph.2009.10.004

Martha TR, Kerle N, van Westen CJ, et al. (2011) Segment optimization and data-driven thresholding for knowledge-based landslide detection by object-based image analysis. IEEE Trans Geosci Remote Sens 49: 4928-4943.
https://doi.org/10.1109/TGRS.2011.2151866

Miandad J, Darrow MM, Hendricks MD, et al. (2020) Landslide Mapping using multiscale LiDAR digital elevation models. Environ Eng Geosci 26(4): 405-425.
https://doi.org/10.2113/EEG-2268

Miura T, Nagai S (2020) Landslide detection with himawari-8 geostationary satellite data: a case study of a torrential rain event in Kyushu, Japan. Remote Sens 12: 1734.
https://doi.org/10.3390/rs12111734

Oreti L, Giuliarelli D, Tomao A, et al. (2021) Object oriented classification for mapping mixed and pure forest stands using very-high resolution imagery. Remote Sens 13: 2508.

https://doi.org/10.3390/RS13132508

Qu F, Qiu H, Sun H, et al.(2020) Post-failure landslide change detection and analysis using optical satellite Sentinel-2 images. Landslides 18(1): 447-455.
https://doi.org/10.1007/S10346-020-01498-0

Şerban RD, Şerban M, He R, et al. (2021) 46-Year (1973–2019) Permafrost landscape changes in the hola basin, northeast china using machine learning and object-oriented classification. Remote Sens 13: 1910.
https://doi.org/10.3390/rs13101910

Syzdykbayev M, Karimi B, Karimi HA (2020) Persistent homology on LiDAR data to detect landslides. Remote Sens Environ 246: 111816.
https://doi.org/10.1016/j.rse.2020.111816

Tehrani FS, Santinelli G, Herrera M (2021) Multi-Regional landslide detection using combined unsupervised and supervised machine learning. Geomatics, Geomat Nat Hazards Risk 12(1): 1015-103.
https://doi.org/10.1080/19475705.2021.1912196

Tran CJ, Mora OE, Fayne JV, et al. (2019) Unsupervised classification for landslide detection from airborne laser scanning. Geosci 9(5):221.
https://doi.org/10.3390/geosciences9050221

Wan S, Jia YY, Lin CY, et al. (2015) Construction of knowledge-based spatial decision support system for landslide mapping using fuzzy clustering and KPSO analysis. Arabian J Geosci 8(2): 1041-1055.
https://doi.org/10.1007/s12517-013-1226-5

Xu Q, Dong XJ, Li WL (2019) Integrated space-air-ground early detection, monitoring and warning system for potential catastrophic geohazards. Geo Spat Inf Sci 44(7): 957-966. (In Chinese)
https://doi.org/10.13203/j.whugis20190088

Yang ZK, We JB, Deng JH, et al. (2021) Mapping outburst floods using a collaborative learning method based on temporally dense optical and SAR data: A case study with the Baige landslide dam on the Jinsha River, Tibet. Remote Sens 13(11): 2205.
https://doi.org/10.3390/rs13112205

Yao X, Li L, Zhang Y, et al.(2017) Types and characteristics of slow-moving slope geo-hazards recognized by TS-InSAR along Xianshuihe active fault in the eastern Tibet Plateau. Nat Hazards 88(3): 1727-1740.
https://doi.org/10.1007/s11069-017-2943-y

Zhang P, Xu C, Ma S, et al.(2020) Automatic extraction of seismic landslides in large areas with complex environments based on deep learning: An example of the 2018 Iburi earthquake, Japan. Remote Sens12: 3992.
https://doi.org/10.3390/rs12233992

Zhao F, Wu X, Wang S (2020) Object-oriented vegetation classification method based on UAV and satellite image fusion. Procedia Comput Sci 174: 609-615.
https://doi.org/10.1016/j.procs.2020.06.132

Zhu Q, Chen L, Hu H, et al. (2020) Deep fusion of local and non-local features for precision landslide recognition. IEEE Access.
https://doi.org/10.48550/arXiv.2002.08547